Thermodynamic properties and p-T phase diagrams of $(NH_4)_3M^{3+}F_6$ cryolites (M^{3+}: Ga, Sc)

Thermodynamic properties and p–T phase diagrams of $(NH_4)_3M^{3+}F_6$ cryolites (M^{3+}: Ga, Sc)

M V Gorev†, I N Flerov† and A Tressaud‡

† L V Kirensky Institute of Physics, 660036 Krasnoyarsk, Russia
‡ Institut de Chimie de la Matière Condensée de Bordeaux–CNRS, Université Bordeaux I,
33608, Pessac Cédex, France

Abstract. Calorimetric and high pressure experiments are used to establish thermodynamic features of $(NH_4)_3M^{3+}F_6$ cryolites with M^{3+}: Ga, Sc as they undergo one and three structural phase transitions, respectively. The heat capacity measurements performed between 80 K and 370 K, using an adiabatic calorimeter, have shown that all phase transitions under study are first order with different closeness to the tricritical point. The total entropy change in the Sc compound connected with the successive transformations is almost equal to the entropy change in the Ga cryolite. The effect of hydrostatic pressure has been studied up to 0.6 GPa, using differential thermographic analysis. The p–T phase diagrams of both cryolites were found to be rather complicated, including triple points. The experimental results are considered as connected with order–disorder phase transitions.

1. Introduction

Crystals with the common formula $A_3M^{3+}F_6$ are usually cubic in an initial high temperature phase and belong to the family of cryolite Na_3AlF_6 (space group $Fm\bar{3}m$, $Z = 4$). This structure is related to the perovskite one and can be derived from it via a cationic ordering between M^{3+} and one third of A^+ ions both of which occupy centres of fluoride octahedra. The remaining A^+ ions are set in vacant sites of coordination number CN = 12. Many crystals of this family are known to undergo structural phase transitions (PTs) connected with either octahedron tilts or/and atom displacements depending on the size and shape of A^+ and M^{3+} ions. As a rule, the PT temperature from a cubic phase is rather high in compounds with monatomic cations and it decreases with increasing size of alkali ions [1–4].

The replacement of the spherical A^+ ion by the tetrahedral ammonium one leads to stabilization of a cubic symmetry which sometimes can be realized even at room temperature [5, 6]. This fact, unusual from a crystallographic point of view, was discussed in terms of the hydrogen bonding, molecular disorder and packing considerations [6].

Some physical properties of ammonium cryolite crystals $(NH_4)_3M^{3+}F_6$ (M^{3+}: Al, Cr, Ga, V, Fe, Sc, In) are significantly affected by the size of the unit cell volume [7]. First, the temperature of transition from the cubic phase increases with increasing radius of M^{3+} ion. Second, crystals with small trivalent ions (M^{3+}: Cr–Fe) exhibit one PT just into a phase with triclinic symmetry [8, 9], whereas the presence in the structure of large M^{3+} ions (Sc, In) leads to a succession of two PTs [7]. The powder x-ray diffraction patterns of both distorted phases of the latter compound were not found to be different by any significant features. The monoclinic

$P2_1/n$ space group was proposed for the lowest temperature phase of $(NH_4)_3ScF_6$ [7] as well as being found for the In compound [10].

Accurate thermodynamic studies using an adiabatic calorimeter were performed only on compounds having an $Fm\bar{3}m$–$P\bar{1}$ PT (M^{3+}: Cr, Ga, V, Fe) [5–8]. It was found that this PT is accompanied by rather large excess entropy change comparing cryolites with alkali cations, which is correlated with an orientational order–disorder PT. For compounds with large M^{3+} ions (Sc, In), which were investigated by differential scanning calorimetry (DSC) [7], the total entropy change associated with succession of two transformations has been found to be almost halved with respect to the entropy of the cryolites mentioned just above. On the strength of these data different models of octahedron disorder in an initial $Fm\bar{3}m$ phase were assumed for compounds with small and large M^{3+} ions.

It is necessary to point out that DSC provides reliable information concerning PT entropy when the transformation is a first order one distant from a tricritical point. To put it differently, the results are more valid when the entropy jump at the PT temperature is the majority of the total entropy change.

For this reason and to determine some subtle details of PTs such as entropy jump, closeness to the tricritical point and hysteresis of PT temperature we have performed reinvestigations of heat capacity on Sc and Ga compounds by adiabatic calorimetry. A portion of these results were presented in [11]. The most important thing was that ammonium scandium cryolite was found to undergo a succession of three structural PTs instead of two observed earlier [7]. A new transformation was detected at $T_3 = 243$ K. In addition, one more interesting point was that the value of total entropy change in $(NH_4)_3ScF_6$ associated with three successive PTs was very close to the excess entropy of the Ga compound undergoing one transformation.

Beside atom substitution the unit cell volume can be decreased by external pressure. So far as we know the pressure effect on PTs in ammonium cryolites has not been studied. Such information could be very useful to throw light on the mechanism of structural transformations. In order to understand the thermodynamic properties of the ammonium cryolite system, the influence of hydrostatic pressure on PTs was studied in the present paper and p–T phase diagrams of Sc and Ga compounds are discussed in combination with the results of the heat capacity measurements.

2. Experimental procedures

Of two possible ways of preparation of cryolites $A_3M^{3+}F_6$ involving ammonium A^+ ions, from aqueous HF solutions or via solid state reaction, we have used the latter one to avoid a possible substitution of fluorine atoms by halide, hydroxyl or H_2O units. The samples $(NH_4)_3ScF_6$ and $(NH_4)_3GaF_6$ were prepared by heating, for several tens of hours, stoichiometric mixtures of NH_4F and metal trifluorides in platinum tubes. These mixtures had been previously ground in controlled atmosphere taking account of the hygroscopy of the starting materials. The reaction temperature 300 °C was reached after a gradual increase.

The heat capacity data have been obtained using an adiabatic calorimeter. Powdered samples with the mass of about 0.45 g were set into the indium container sealed in helium atmosphere. Details of the experimental procedure were presented in [11].

High pressure investigations have also been performed on powdered samples which have been used for calorimetric studies. The variation of PT temperatures was measured by means of differential thermal analysis (DTA) [12]. Hydrostatic pressure up to 0.6 GPa was generated in a DTA vessel of piston-and-cylinder type associated with the multiplier. Silicon oil was used as the pressure-transmitting fluid. The germanium–copper thermocouple was utilized as

a differential device owing to its high sensitivity and because of the good thermal conductivity of Ge. It has allowed us to detect clearly the DTA signal before its dispersion through the silicon oil. Quartz as a reference substance and a small copper container filled with powdered sample were fixed with a glue onto two thermocouple junctions.

Pressure and temperature were measured with a manganin gauge and copper–constantan thermocouple, respectively, with inaccuracy about $\pm 10^{-3}$ GPa and ± 0.3 K. Registration of heat anomalies associated with PTs was performed with increasing as well as decreasing pressure.

3. Experimental results

3.1. Heat capacity

We are going to discuss thermodynamic properties of ammonium cryolites which are associated with PTs. In this connection only the excess part of both heat capacity and entropy is analysed. In figures 1(a) and 1(b) one can see the difference ΔC_p between the total and normal (lattice) heat capacities for $(NH_4)_3ScF_6$ and $(NH_4)_3GaF_6$, respectively. The latter part was determined from smoothed interpolation of the molar heat capacity curves below and above PT. The most important features showing up from $\Delta C_p(T)$ curves are as follows.

  (i) Three heat capacity peaks were found in $(NH_4)_3ScF_6$. Some thermodynamic parameters derived from the calorimetric data are given in table 1. The PT temperatures T_1 and T_2 agree satisfactorily with those reported earlier [7]. The connection of the heat capacity anomaly at T_3 with structural transformation was recently confirmed by polarizing-optic observations on a small oriented plate [13]. In calorimetric measurements all PTs in scandium cryolite were found to be first order ones followed by both the temperature hysteresis δT_i and the enthalpy jump (latent heat) δH_i. Because of the widely separated PT temperatures there is hardly any overlap of the pre- and post-transition effects with each other (figure 1(a)).

Table 1. Thermodynamic parameters of the PTs in some ammonium cryolites.

	$(NH_4)_3ScF_6$		$(NH_4)_3GaF_6$	
	[a]	[7]	[a]	[7]
T_1 (K)	330.8 ± 0.2	330	249 ± 0.2	246.1 ± 0.1
δT_1 (K)	1.8 ± 0.2	—	0.84 ± 0.20	—
δH_1 (J mol^{-1})	3820 ± 370	—	2690 ± 190	—
ΔS_1 (J mol^{-1} K^{-1})	13.36 ± 0.95	10.6	23.0 ± 1.6	21.3
$\Delta V_1 / V_1$ (%)	-0.15	—	-0.10	—
T_2 (K)	293.4 ± 0.2	291	—	—
δT_2 (K)	0.52 ± 0.15	—	—	—
δH_2 (J mol^{-1})	160 ± 20	—	—	—
ΔS_2 (J mol^{-1} K^{-1})	6.73 ± 0.48	2.2	—	—
$\Delta V_2 / V_2$ (%)	0.03	—	—	—
T_3 (K)	243.1 ± 0.3	—	—	—
δT_3 (K)	7.1 ± 0.3	—	—	—
T_3 (K)	7.1 ± 0.3	—	—	—
δH_3 (J mol^{-1})	170 ± 25	—	—	—
ΔS_3 (J mol^{-1} K^{-1})	0.7 ± 0.1	—	—	—
$\Delta V_3 / V_3$ (%)	0.04	—	—	—

[a] This work and [11].

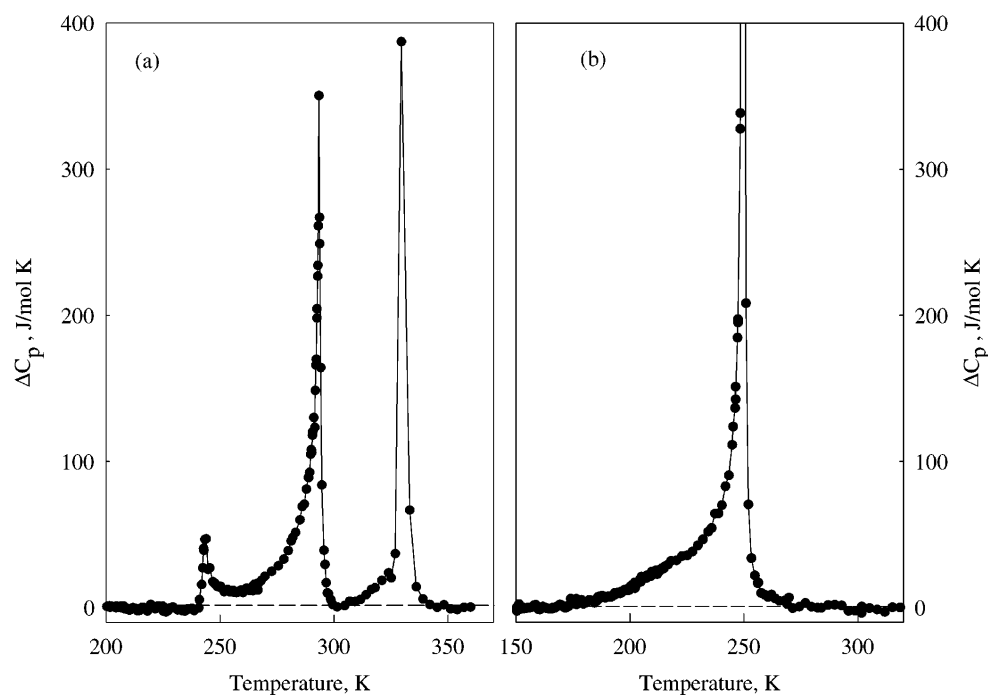**Figure 1.** Excess heat capacity of $(NH_4)_3ScF_6$ (a) and $(NH_4)_3GaF_6$ (b).

(ii) A heat capacity anomaly connected with PT in the $(NH_4)_3GaF_6$ sample, studied in the present paper, was found at T_1 which is about 3.5 K above compared with previous results [7]. Perhaps this difference is not strange or large because fluorides of perovskite-like structure (elpasolites, cryolites, layered perovskites etc) are rather sensitive to points such as method of preparation, degree of stoichiometry and so on. From continuous heating and cooling measurements both the enthalpy jump and the hysteresis behaviour of the phase change were detected (table 1). In spite of the first order PT the excess heat capacity of the low temperature phase extends over a wide temperature range below T_1.

3.2. Effect of hydrostatic pressure

The resultant pressure–temperature phase diagram of $(NH_4)_3ScF_6$ is shown in figure 2(a). The PT temperature T_1 decreases while the T_2 temperature increases with increasing pressure. Both phase boundaries are almost linear and the pressure coefficients of the T_1 and T_2 temperatures are $-(16.4 \pm 1.3)$ K GPa^{-1} and (57.5 ± 1.7) K GPa^{-1}, respectively. As a result, the temperature region of phase 2 narrows as pressure increases and disappears at triple point 1 at $p_{1tr} = 0.52$ GPa and $T_{1tr} = 323$ K. For pressure above p_{1tr}, phase 1 ($Fm\bar{3}m$) directly transforms to phase 3. The pressure coefficient of the $Fm\bar{3}m$–3 transformation is the same as for the $Fm\bar{3}m$–2 one.

The PT temperature T_3 increases linearly with pressure increase. The value of T_3 shift under pressure is (59.9 ± 1.2) K Gpa^{-1}.

The phase diagram of $(NH_4)_3GaF_6$ is rather complicated too (figure 2(b)). Two triple points and two high-pressure phases were found during measurements from 100 to 300 K and from 0 to 0.6 GPa. PT $Fm\bar{3}m$–2′ occurs in a rather narrow pressure region from
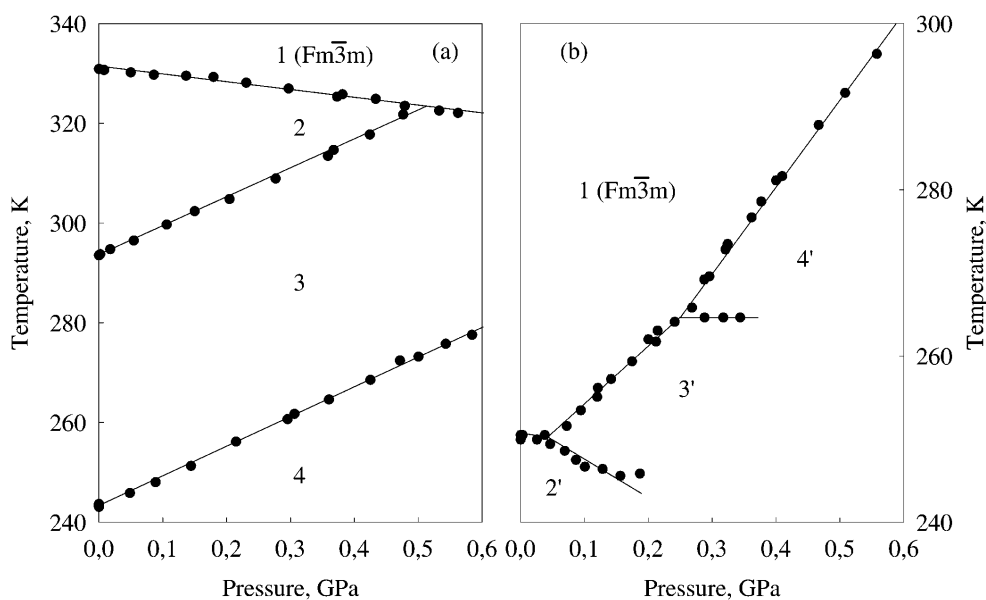
Figure 2. *p–T* phase diagrams of (NH$_4$)$_3$ScF$_6$ (a) and (NH$_4$)$_3$GaF$_6$ (b).

0 to 0.045 GPa. The temperature T_1 decreases with increase in pressure with a rate of $-(12.1 \pm 20.0)$ K GPa^{-1}. The coordinates of the first triple point are as follows: $T_{1tr} = 250$ K, $p_{1tr} = 0.045$ GPa. The phase boundaries $Fm\bar{3}m$–3$'$ and 3$'$–2$'$ are linear with the following slopes: $dT_{1-3'}/dp = (73.1 \pm 5.5)$ K GPa^{-1} and $dT_{3'-2'}/dp = -(22.5 \pm 15.6)$ K GPa^{-1}. The second triple point was taken to be at $T_{2tr} = 265$ K and $p_{2tr} = 0.25$ GPa. The $Fm\bar{3}m$–4$'$ PT temperature increases linearly with increasing pressure with a rather large rate of $dT_{1-4'}/dp = (101.3 \pm 2.7)$ K GPa^{-1}. The boundary between phases 4$'$ and 3$'$ is almost pressure independent: $dT_{4'-3'}/dp \approx 0$ K GPa^{-1}.

Because of very rapid decrease and smearing with pressure the DTA anomalies associated with PTs 3$'$–2$'$ and 4$'$–3$'$ were detected in a narrow pressure range.

4. Discussion

The excess entropy ΔS_i has been evaluated by both an integration of the $(\Delta C_p/T)(T)$ function and the addition of the discontinuous part at the PT temperature determined as $\delta S_i = \delta H_i/T_i$ (table 1). The temperature behaviour of the anomalous entropy for both cryolites studied is shown in figure 3. It is necessary to point out that the values ΔS_1 in the Ga compound determined in the present measurements and in [7] are in good agreement (table 1).

The most valid way to compare PTs from thermodynamic point of view is to consider their degree of proximity to the tricritical point. This value can be evaluated, for instance, by a relation between an entropy jump at PT temperature and a total entropy change $\delta S_i/\Delta S_i$.

Although the discontinuous parts of the anomalous entropy at T_1 in both cryolites studied are almost equal to each other $\delta S_1 \approx 11$ J mol K^{-1}, the PT from the cubic phase in the Ga compound is much closer to the tricritical point ($\delta S_1/\Delta S_1 = 0.46$) than in the Sc one ($\delta S_1/\Delta S_1 = 0.86$).

Two low temperature PTs in the latter cryolite are significantly different from this point
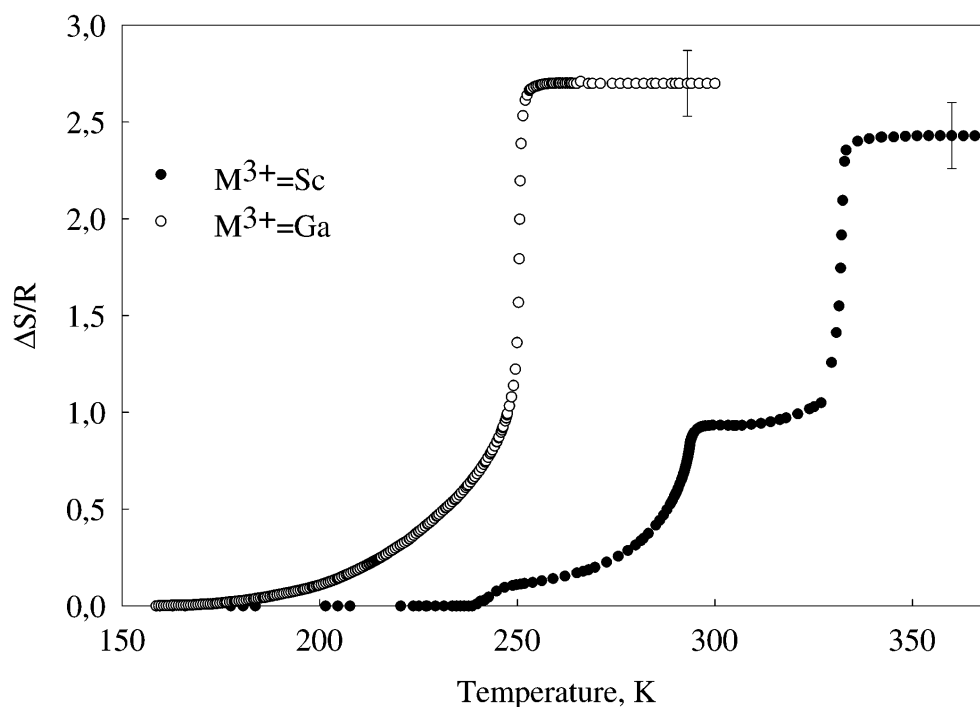
Figure 3. Transition entropies of ammonium cryolites $(NH_4)_3M^{3+}F_6$.

of view: $\delta S_2/\Delta S_2 = 0.08$ and $\delta S_3/\Delta S_3 = 1$. The PT at T_2 is very close to the tricritical point and this is the reason why the entropy change ΔS_2, obtained in the present work by means of an adiabatic calorimeter, is three times larger than that found in DSC measurements [7] (table 1). There is no such large difference between the results of both measurements for entropy at T_1 where the PT is relatively far from the tricritical point. Rather large temperature hysteresis δT_3 (table 1) and the value $\delta S_3/\Delta S_3$ allow us to consider the PT at T_3 as a real first order transformation.

Using the Clausius–Clapeyron relation $dT_i/dp = \delta V_i/(V_i \delta S_i)$ one can evaluate a jump of the unit cell volume at the PT temperature. It is seen (table 1) that all PTs are characterized by a small volume change, in spite of the very large value $\delta S/\Delta S$ for some of them. It is rather difficult to detect experimentally such a weak effect. An x-ray study of the thermal evolution of the unit cell parameters of $(NH_4)_3ScF_6$ near T_1 was performed in [7]. In spite of a great abrupt splitting of the unit cell parameters, no significant change in volume was observed.

Let us consider the p–T phase diagrams in association with calorimetric data. The linear pressure dependence of PT temperatures in $(NH_4)_3ScF_6$ (figure 2(a)) allows us to suppose that the 1–3 and 3–4 phase boundaries approaching each other with increasing pressure meet at the 1–3–4 triple point. The parameters of this point are as follows: $T_{2tr} \approx 312$ K, $p_{2tr} \approx 1.2$ GPa. Consequently, at pressures higher than p_{2tr} Sc cryolite undergoes one PT 1–4. On the other hand, as may be seen in figure 3, the total entropy change $\sum \Delta S_i$ connected with the succession of PTs in Sc cryolite agrees with the value ΔS_1 for the Ga compound, to within the experimental error of the entropy measurement. All cited experimental facts allow us to suppose that PT 1–4 in Sc cryolite could be the same as in the Ga compound at ambient pressure. Really, according to [13] the most probable symmetry of phase 4 in the former compound is triclinic as suggested

for the phase $2'$ in the latter one [9]. This means that the p–T diagram of (NH$_4$)$_3$GaF$_6$, having less cubic unit cell volume [7], can be presented as an extension of that for (NH$_4$)$_3$ScF$_6$. It is interesting to analyse the part of the phase diagram for the Ga compound at pressures higher than $p = p_{1tr}$. Further decrease of the unit cell volume under pressure is followed by the appearance of two high-pressure phases $3'$ and $4'$ (figure 2(b)). This fact could be considered in connection with the Al compound having the smallest unit cell volume among the ammonium cryolites [7] and undergoing at ambient pressure two PTs [6]. Of course to be sure in such an assumption it is necessary to study at least the p–T diagram of (NH$_4$)$_3$AlF$_6$ and the symmetry of the high pressure phases in (NH$_4$)$_3$GaF$_6$.

Taking into account the rigidity of M^{3+}F$_6$ ionic groups and the ionicity of bondings within the structure [14–16], the entropy change in ammonium cryolites undergoing $Fm\bar{3}m$–$P\bar{1}$ (M^{3+}: Ga, Cr, V, Fe) was interpreted as associated with an order–disorder transformation for both NH$_4^+$ and (MF$_6$)$^{3-}$ ions [5–7]. The orientational disorder of fluorine octahedra in a cubic phase was considered as connected with 192l position of fluorine atoms with a respective occupancy fraction of $1/8$. Of two ammonium ions occupying different sites 8c and 4b only the latter is disordered, having two distinct orientations [5, 17]. Thus the total entropy connected with structural distortions due to the ionic ordering is given by the sum of contributions from the ammonium and hexafluorometallate(III) ions: $\Delta S = R(\ln 2 + \ln 8) = 2.77R$. This value is in good agreement with entropies found experimentally in [5, 7] and in the present paper for ammonium cryolites with M^{3+}: Ga, V, Fe. The model of PT $Fm\bar{3}m$–$P\bar{1}$ as connected with simultaneous ordering of octahedra and tetrahedra was proved by the results of the NMR studies of the Ga compound [18] where the discontinuity in the spin–lattice relaxation time for the proton and fluorine nucleus was detected at PT point.

The total entropy in the Sc cryolite (figure 3) is compatible with the entropy of the order–disorder model too. However only PTs at T_1 and T_2 can be considered as associated with the ordering process according to the values of entropy close to $R \ln 8$ and to $R \ln 2$, respectively. This supposition is proved by the NMR results for (NH$_4$)$_3$InF$_6$ [18] which also seemed, based on the data [7, 19], to undergo a succession of three PTs. The anomalous temperature behaviour of the spin–lattice relaxation times T_{1H} and T_{1F} were detected only at T_1 and T_2. So at least in the Sc cryolite the entropy change at PT from the cubic phase is connected with the ordering of ammonium tetrahedra ($R \ln 2$) and with partial ordering of octahedra ($R \ln 4$). Final ordering of the octahedra results from the PT at T_2 ($\Delta S_2 \approx R \ln 2$). The third PT is the first order one followed by great thermal hysteresis and small entropy change and so it is not an order–disorder transformation. It can be supposed that both phases 3 and 4 are completely ordered variants of the initial phase $Fm\bar{3}m$. To obtain information about the mechanism of the third PT and the relation between symmetries of phases 3 and 4 the structural studies are needed.

Acknowledgments

References

[1] Holm J L 1965 *Acta Chem. Scand.* **19** 261
[2] Grannec J, Champarnaud-Mesjard J C, Cousseins J C and Gaudreau B 1972 *Rev. Chim. Miner.* **9** 569
[3] Chassaing J 1968 *Rev. Chim. Miner.* **5** 1115
[4] Kozak A, Almai M and Samouel M 1979 *Rev. Chim. Miner.* **16** 441

[5] Moriya K, Matsuo T, Suga H and Seki S 1977 *Bull. Chem. Soc. Japan* **50** 1920
[6] Moriya K, Matsuo T, Suga H and Seki S 1979 *Bull. Chem. Soc. Japan* **52** 3152
[7] Tressaud A, Khairoun S, Rabardel L, Kobayashi T, Matsuo T and Suga H 1986 *Phys. Status Solidi* a **96** 407
[8] Kobayashi K, Matsuo T, Suga H, Khairoun S and Tressaud A 1985 *Solid State Commun.* **53** 719
[9] Epple M 1978 *Thesis* University of Tübingen
[10] Schwarzman S 1966 *Fortschr. Mineral.* **42** 231
[11] Flerov I N, Gorev M V and Ushakova T V 1999 *Fiz. Tverd. Tela* **41** 523
[12] Flerov I N and Gorev M V 1992 *Fiz. Tverd. Tela* **34** 2555
[13] Melnikova S V 1999 private communication
[14] Shearer-Turrell S, Tressaud A and Portier J 1970 *J. Mol. Struct.* **7** 289
[15] Knop O, Westerhaus J, Falk M and Massa W 1985 *Can. J. Chem.* **63** 3328
[16] Pebler J, Herdtweck E, Massa W and Schmidt R 1983 *Stud. Inorg. Chem.* **3** 501
[17] Roloff A, Trinschek D and Jansen M 1995 *Z. Anorg. Allg. Chem.* **621** 737
[18] Sasaki A, Furukawa Y and Nakamura D 1989 *Ber. Bunsenges. Phys. Chem.* **93** 1142
[19] Vecher R A, Volodkovich L M, Petrov G S and Vecher A A 1985 *Thermochim. Acta* **87** 377